

Porosity estimation in deep-water slope-channel system using seismic inversion model: A case study from the Nile Delta Basin, Egypt

Ramy EID¹ , Mohamed EL-ANBAAWY² , Adel EL-TEHIWY^{2,*} 

¹ Rashid Petroleum Company (Rashpetco), Building 18, New Maadi, 1073, Cairo, Egypt

² Department of Geology, Faculty of Science, Cairo University, Giza, 12613, Egypt

Abstract: The area of study is a Pliocene gas field, located in the Eastern portion of the West Nile Delta Deep Marine Concession (WDDM) offshore Egypt. The primary aim of this study is to establish a methodology for direct porosity estimate from 3D post-stack inversion (Z_p) and assess its reliability. Porosity estimation from seismic inversion is a commonly used technique in geophysics to predict subsurface porosity from seismic data. Seismic inversion is the process of converting seismic reflection data into a quantitative representation of subsurface properties. Seismic inversion methods aim to relate the seismic response (amplitude, phase, frequency content) to rock properties such as porosity. The inversion process typically involves the following steps: Acoustic impedance inversion from seismic data is a widely utilized technique in reservoir characterization. In cases where well penetrations are limited, the resulting impedance section can be employed to predict reservoir parameters, including porosity. However, the relationship between acoustic impedance (AI) and porosity is influenced by the lithofacies and requires geological interpretation. To construct a porosity map and porosity static model, a comprehensive methodology was developed, capitalizing on the expected porosity volumes. By applying cut-offs to shear and acoustic impedance logs, categorical facies or fluid classes were established. The mean porosity for each lithofacies category is determined from the porosity logs of the wells under study. The inverted porosity model is validated against well log data or other independent measurements like core porosity to assess its accuracy and reliability. If necessary, additional adjustments or calibration may be performed to improve the porosity estimation. Subsequently, a final trend porosity volume was generated to estimate the porosity in areas distant from the study wells by establishing a correlation between average porosity values and acoustic impedance. This process of creating a porosity map will significantly mitigate drilling uncertainties going forward.

Key words: porosity estimation, deep-water slope-channel system, Simian Field, Nile Delta basin, seismic inversion model

*corresponding author, e-mail: aabdelmoneim@sci.cu.edu.eg

1. Introduction

Simian Field is located at the north-western margin of the offshore Nile Delta, approximately 120 km from Alexandria shoreline. The field lies in the West Delta Deep Marine (WDDM) concession. It lies at the cross of latitudes $31^{\circ}46'$ & $32^{\circ}10' 48.085''$ N and longitudes $30^{\circ}10'$ & $30^{\circ}49' 21.733''$ E (Fig. 1). Porosity prediction from seismic inversion enables the prediction of porosity distribution away from drilled wells, improves the technical and economic characterization of discovered reservoirs, and provides much more information than standard seismic interpretation in the search for new hydrocarbon fields (Aly et al., 2019). The relevance of quantitative seismic interpretation to reservoir characterisation is increasing as seismic data re-

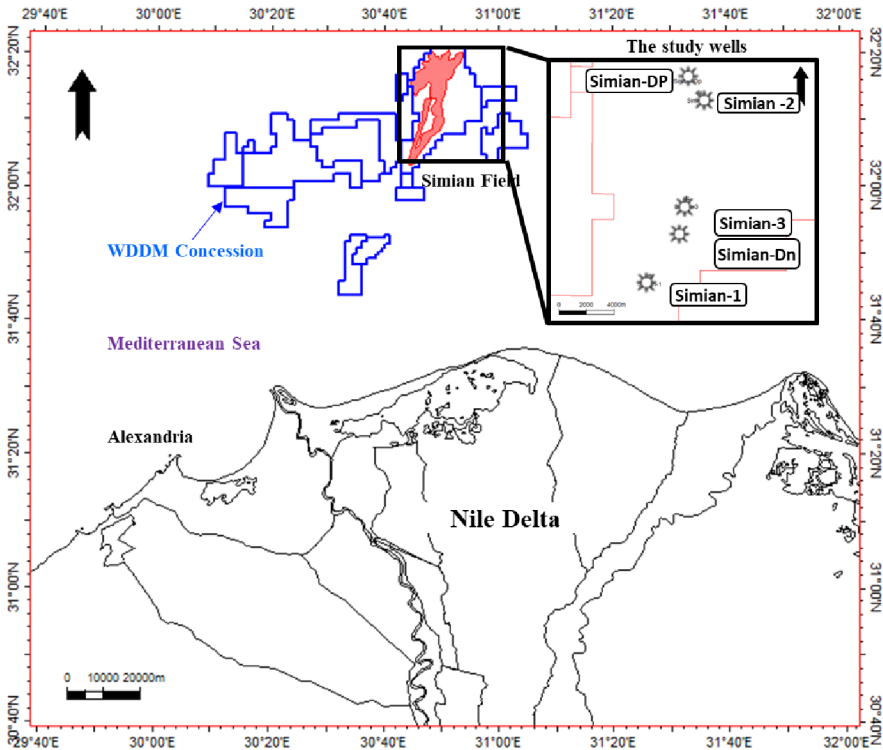


Fig. 1. The location map shows WDDM concession and a pop-up map showing the Simian Field and the study wells Simian-1, Simian-2, Simian-3, and Simian-DP.

liability increases due to recent improvements in acquisition and processing methods. These improvements increase the effectiveness of the multidisciplinary data integration methods in reducing the operational risks associated with reservoir exploration and production. Geology, geophysics, and engineering approaches are additionally necessary for a better comprehension of the reservoir properties. The estimated porosity trends could be revealed in the unknown reservoir geological model. The available data is post-stack seismic cube and five well penetrations with their complete set of logs such as; resistivity, gamma ray and density logs.

The early 1980s saw the advent of wavelet amplitude and phase spectra extraction methods. This led to the development of the post-stack AI inversion technique (*Lindseth, 1979*). High resolution inversion results improved the interpretation and decreased drilling risk (*Pendrel, 2006*). In practice, a lot of methods are used to perform post-stack AI inversion. Post-stack inversion can be subdivided into two main approaches: band-limited (iterative) inversion and broad-band inversion, which in its turn includes the model-based inversion (deterministic inversion) as discussed by *Russell and Hampson (1991)*. *Abbas et al. (2019)* integrated the seismic interpretation with the petrophysical data and the seismic attributes; Moreover, *Abdolahi et al. (2022)*, studied Seismic inversion as a reliable technique for anticipating the porosity and facies delineation.

A machine learning – a novel approach of well logs similarity based on synchronization measures to predict shear sonic logs was investigated by *Ali et al. (2021)*; Classification of reservoir facies using well logs and 3D seismic attributes for prospect evaluation and field development (*Ashraf et al., 2019*). An integrated sedimentological, rock typing, image logs, and artificial neural networks analysis for reservoir quality assessment of the heterogeneous fluvial-deltaic Messinian Abu Madi reservoirs (*El-Gendy et al., 2022*), *Tonn (2002)* studied the neural network seismic reservoir characterization in a heavy oil reservoir.

Predicting a trustworthy porosity is a key component of reservoir modelling for slope channel gas fields due to the complex porosity distribution in clastic reservoirs. Reservoir elastic characteristics are evaluated during the seismic inversion process.

Due to the complex porosity distribution in clastic reservoirs, predicting a reliable porosity is a crucial part of reservoir modelling for slope channel

gas fields. During the seismic inversion process, reservoir elastic properties are assessed. It is possible to execute a fluid classification using these inverted elastic characteristics, and as a results of this stage, porosity volumes are produced in collaboration with the field geologists to be utilised as input in the geological modelling process. It can also be done, with certain restrictions, in locations where such reliable data are notably absent. Pre-stack inversion, post-stack inversion, and geostatistical seismic inversion are all possible (Helal et al., 2014). They concluded that the choice of a particular inversion technique is largely influenced by the properties of the subsurface depositional facies. For all methods, estimated seismic wavelets from the seismic reflection data are necessary.

The statistical wavelet (Helal et al., 2014), phase, and frequency are typically estimated using a reflection coefficient series from a stratigraphic control well with available sonic and density logs that is located inside the seismic survey field. A precise connection between the impedance log and seismic data is necessary for accurate wavelet estimate. Phase and/or frequency aberrations in the estimation wavelet may be the result of well-tie errors. The most typical step following wavelet identification is to eliminate wavelet tuning and interference effects, which results in a high-resolution depiction of the acoustic impedance volume, or the principal seismic velocity multiplied by the bulk density. The results of the inversion are next convolved with the seismic wavelet to create artificial seismic traces that are subsequently updated and compared repeatedly to the original (measured) traces (Helal et al., 2014). Barakat and Dominik (2010) conducted seismic studies on the Messinian rocks in the Onshore Nile Delta. Challenges of the seismic image resolution for gas exploration in the East Mediterranean Sea and decoding of seismic data for complex stratigraphic traps revealed by seismic attributes analogy in Yidma/Alamein concession area Western Desert, Egypt was illustrated by Barakat et al. (2021) and El-Nikhely et al. (2022). The present interpretation is revealed using the available data in each studied well.

2. Geological setting

Simian Field is a Pliocene gas field located in the Eastern part of the West Delta Deep Marine (WDDM) concession, with water depths ranging be-

tween 500 to 1500 m. The WDDM concession is affected by major tectonic events that shaped the present-day alignment of the northeast, southwest trending Rosetta fault, and the east-northeast, west-northwest Nile Delta offshore anticline (NDOA) (*Eid et al., 2020*). These structural features have been shaped due to the wrench tectonics (*Sehim et al., 2002*) resulting from the rotational movement of the African plate towards the Eurasian plate (*Dolson et al., 2005*). The Nile delta region occupies a key position within the plate tectonic development of the East Mediterranean and Levantine basins. It lies on the northern margin of the African plate which extends from the subduction zone adjacent to the Cretan and Cyprus arcs to the Red Sea rift basin which was rifted apart from the Arabian plate (*Cowan et al., 1998*).

The majority of deep-water hydrocarbon reserves have so far been discovered in reservoirs between the Cenozoic and Mesozoic ages. Nearly 90% of these reserves are in deep-water sandstone reservoirs. The top seal is widespread as mud rock deposited in deep marine environments. However, this top seal is insufficient because the seal integrity is a crucial concern and is seen as a significant risk in deep-water environments. In deep marine environments, source rock potentiality is considerable. The ages of most source rocks range from the Mesozoic to the Cenozoic (*Dolson et al., 2001*). According to *Mitchum et al. (1993)*, and *Duval et al. (1998)* the source rocks were considered as lacustrine deposits, terrigenous deltaic deposits, and/or deep marine deposits. Therefore, the variety of hydrocarbon composition includes biogenic gas, waxy, sulfur-rich oil, and asphaltenes (*Weimer and Slatt, 2004*). Simian Field represents a channel complex deposited on the Nile delta slope in the early Pliocene within El-Wastani Formation package (*Othman et al., 2020*). The stratigraphic succession of Simian Field is composed of Bilqas, Mit Ghamr, and El-Wastani formations (Fig. 2). Simian reservoir mainly belongs to El-Wastani Formation.

3. Data and methods

The Pliocene reservoirs of the WDDM and Rosetta concessions are well-defined on 3-D seismic data, originally acquired in 1996 (*Samuel et al., 2003; Cross et al., 2009*). The acquisition of a new seismic survey in 2006 was required because of the fields' increasing maturity and the requirement

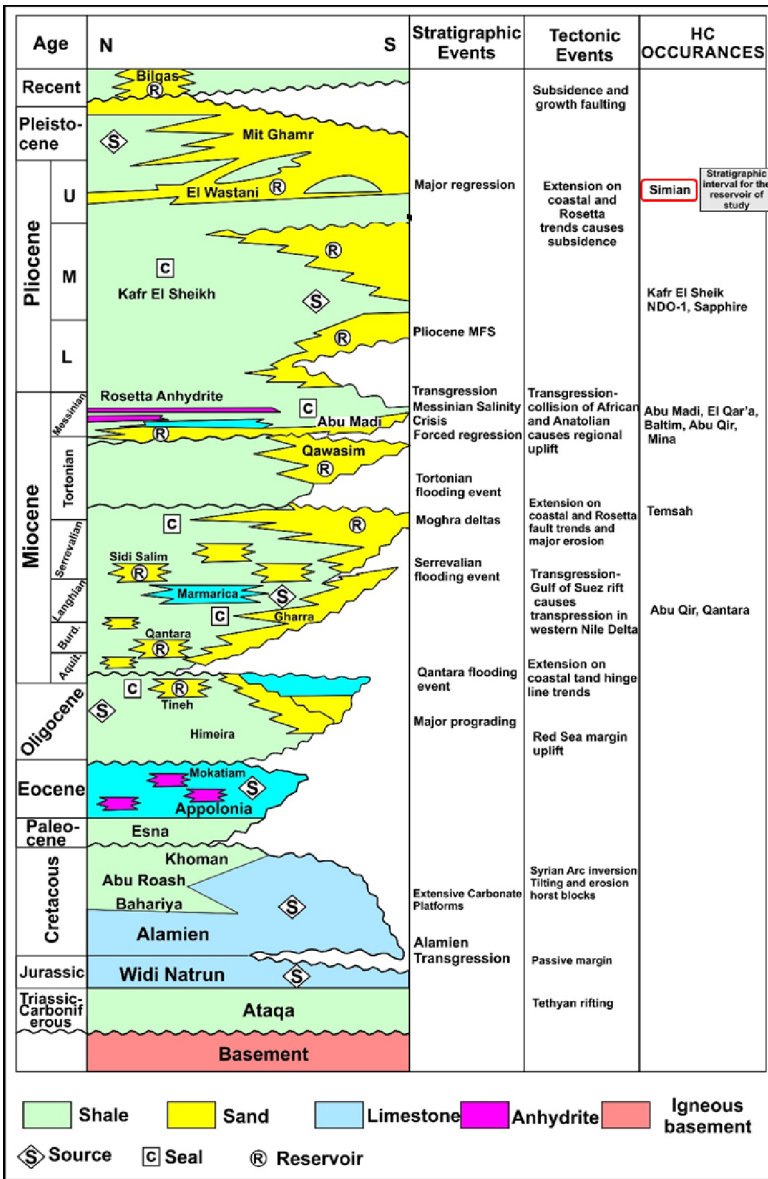


Fig. 2. Nile Delta tectonostratigraphic displaying the key stratigraphic, and tectonic events modified after Deibis et al. (1986), Cowan et al. (1998), Dolson et al. (2005), Wood et al. (2012), and Eid et al. (2020).

for a better resolution development survey. This development survey, which was intended to serve as a baseline for the four-dimensional survey and covers an area of roughly 1800 km², has enabled subsequent infill drilling and greater resolution static models (Cross et al., 2009).

The method begins, Fig. 3, porosity prediction workflow, with statistical wavelet extraction from the seismic data in the study area as the first step of the inversion process in the vicinity of the study wells (Fig. 4) using Hamson Russel software. The log-to-seismic correlation (the well to seismic tie) process was finished when a satisfactory wavelet was extracted, and top and base the reservoir were chosen. The post-stack inversion then proceeded to determine the initial model (Fig. 5). An initial layered elastic model defined in the time domain serves as the foundation for the 3D model-based inversion approach (Coulon et al., 2006). In order to find a global solution that concurrently optimizes the match between the seismic and the corresponding synthetics generated by convolution with full Zoeppritz reflectivity equations. The model was given a 10-Hz, low-pass filter for two purposes; the low frequencies absent from the stacked seismic data had to first be recovered using the low-frequency impedance trend. Moreover, as impedances above 10 Hz should only be derived from seismic data, this frequency range should be excluded from the well-log data when creating the initial model. Because the spectrum of the stacked seismic section provided no data below this frequency, the 15-Hz cut-off was used. Iterations

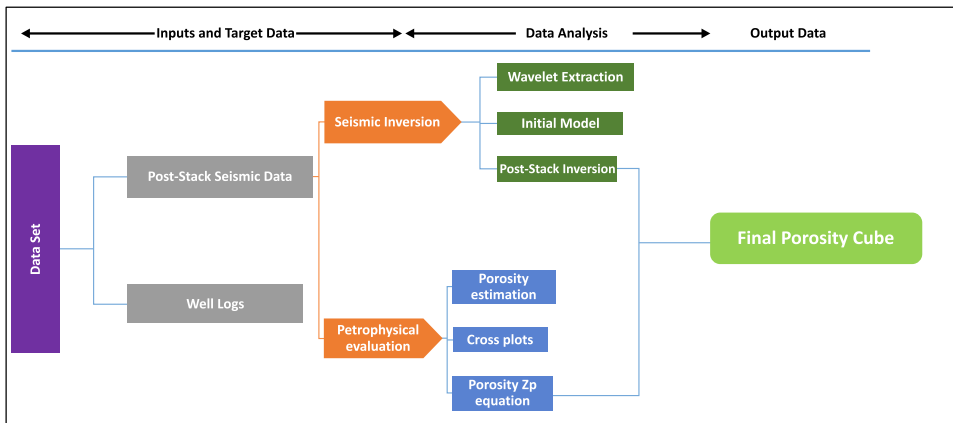


Fig. 3. Porosity prediction workflow.

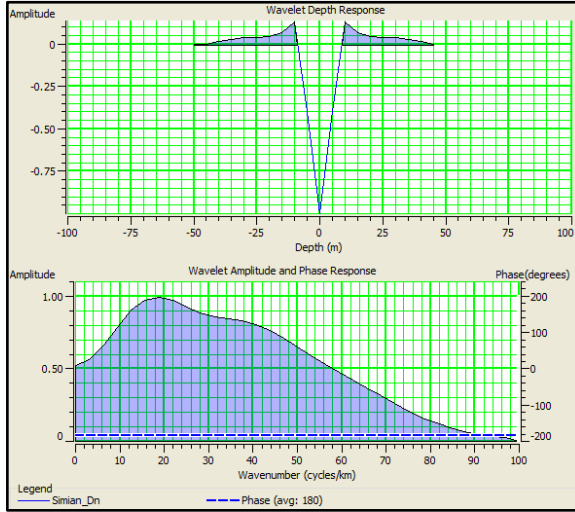


Fig. 4. Statistical wavelet estimation from seismic and Simian Dn well, with depth response on top and respective amplitude spectrum on the bottom. The phase is constant 180 degrees for the wavelet.

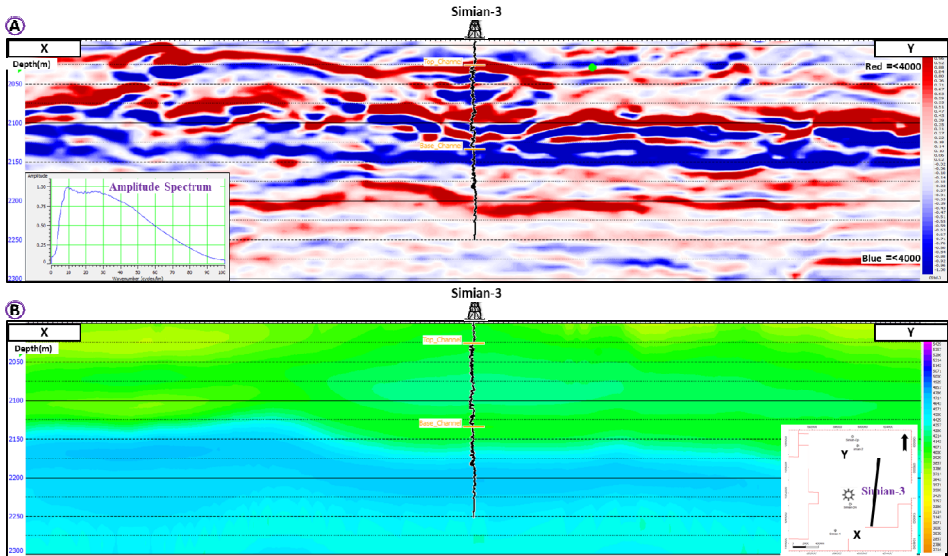


Fig. 5. (A) Representative seismic section in the field of study area range of 2000–3300 m; (B) cross-section of the low-frequency initial acoustic impedance model. (Hot colours represent low amplitude and pale colour background), the displayed log is GR.

were utilized in model-based inversion to improve the similarity of the real and synthetic seismic traces. The model's average impedance, which was represented by filtered well impedances, was used as the reference point for the impedance change restrictions.

Following that, a cross plot between shear impedance (Z_s) and compressional impedance (Z_p) at the well locations was conducted to distinguish shale from non-shale areas (gas and water sands) using techlog software. The cut-off values were employed to distinguish between reservoir and non-reservoir facies. The Z_p Values below 3980 represent gas sand, while the range of 3950–4800 corresponds to shale, and values above that indicate water sand. These cut-off values were determined based on the reservoir's properties. Additionally, a useful porosity vs. P-impedance relationship was constructed from the wells to produce Eq. (2), such equation for transforming the impedance cube into a porosity cube for use in the building of reservoir static models.

4. Results

This section displays the findings of the lithofacies classification and elastic inversion performed over the research region, emphasizing how these outcomes combine data for reservoir characterization and geological modelling. The total porosity in the location of the study wells was calculated using the porosity Eq. (1) (*Schlumberger, 1987*) which revealed from the density logs in Simian-3, Simian-Dp and Simian-2 wells (Fig. 6). After that the volume of shale was calculated to obtain the effective porosity from the calculated total porosity. The porosity values range from 0.15 (15%) to 0.30 (30%) as shown in Fig. 6. The depicted figure illustrates the frequency distribution of porosity for the wells under study. It reveals that both Simian-3 and Simian-2 exhibit bimodal porosity ranges, except for Simian-Dp, which displays a unimodal distribution of porosity.

$$\Phi = \frac{\rho_{ma} - \rho_b}{\rho_{ma} - \rho_f}, \quad (1)$$

where Φ = porosity, ρ_{ma} = matrix density (2.65), ρ_b = formation bulk density (log value), ρ_f = density of the fluid saturating the rock (1.07).

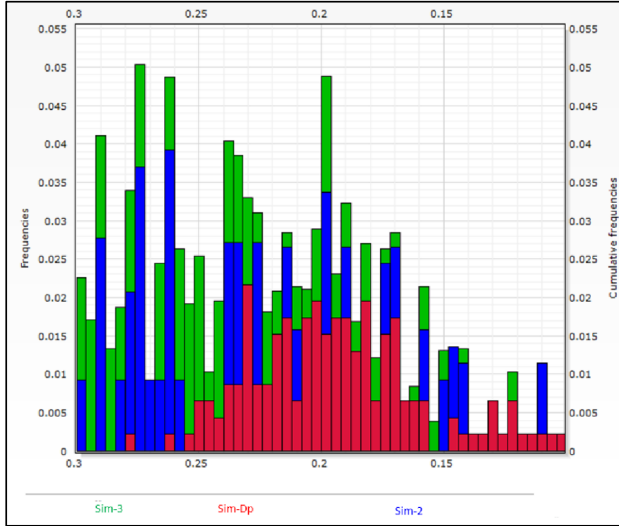


Fig. 6. Average calculated effective porosity histogram for the wells in the study area.

A common way to extract porosity from the seismic data is to use the acoustic impedance inversion results, one can estimate the porosity from the inverted AI, using a mathematical relation between the AI and the porosity derived from well log (Fig. 7), Eq. (2). According to the conclusions of rock physics, there should be a correlation between acoustic impedance and porosity in the well data. In agreement with these conclusions, the revealed results from cross plotting (Fig. 7), the acoustic impedance is strongly correlated to the porosity. In order to convert the acoustic impedance data to porosity, the acoustic cube should be classified into reservoir sandy facies and non-reservoir muddy facies as shown in (Fig. 8). A cross-plot analysis was conducted using shear and compressional impedance to delineate the boundary between reservoir and non-reservoir facies. This analysis helped establish the acoustic impedance cut-off for separating the different facies as each facies has its range from acoustic impedance (Fig. 8). An arbitrary seismic line was taken through the study area to illustrate the inverted acoustic impedance versus the raw seismic data (Fig. 9). Root mean square amplitude from the post stack seismic was used to map the distribution of the reservoir facies in the area, which represent slope channel features (Fig. 10).

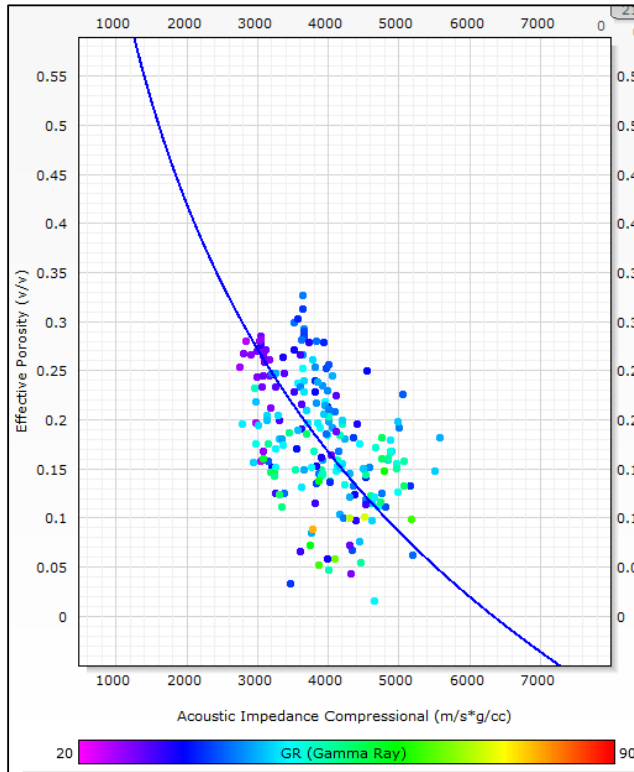


Fig. 7. Cross plot between the target log (effective porosity) and the seismic attribute (AI) for Simian-3, Simian-Dn, and Simian-Dp wells.

Porosity prediction Eq. (2) from the cross plot in Fig. 6 as a best fit regression equation:

$$\text{Effective Porosity} = -0.837 \cdot \log_{10}(\text{Acoustic Impedance}) + 3.182. \quad (2)$$

The obtained porosity cube from the acoustic impedance relationship demonstrated the spatial distribution of the porosity in reservoir units and the areas which have a good trend of the porosity (Fig. 11). Figure 12 depicts the seismic-derived porosity overlaid by the calculated porosity log, providing a visual representation of the relationship between the two. By revealing details about the reservoir’s spatial variation distant from the existing well’s control, seismic porosity prediction might enhance reservoir characterization. Seismically derived maps and volumes have a vertical

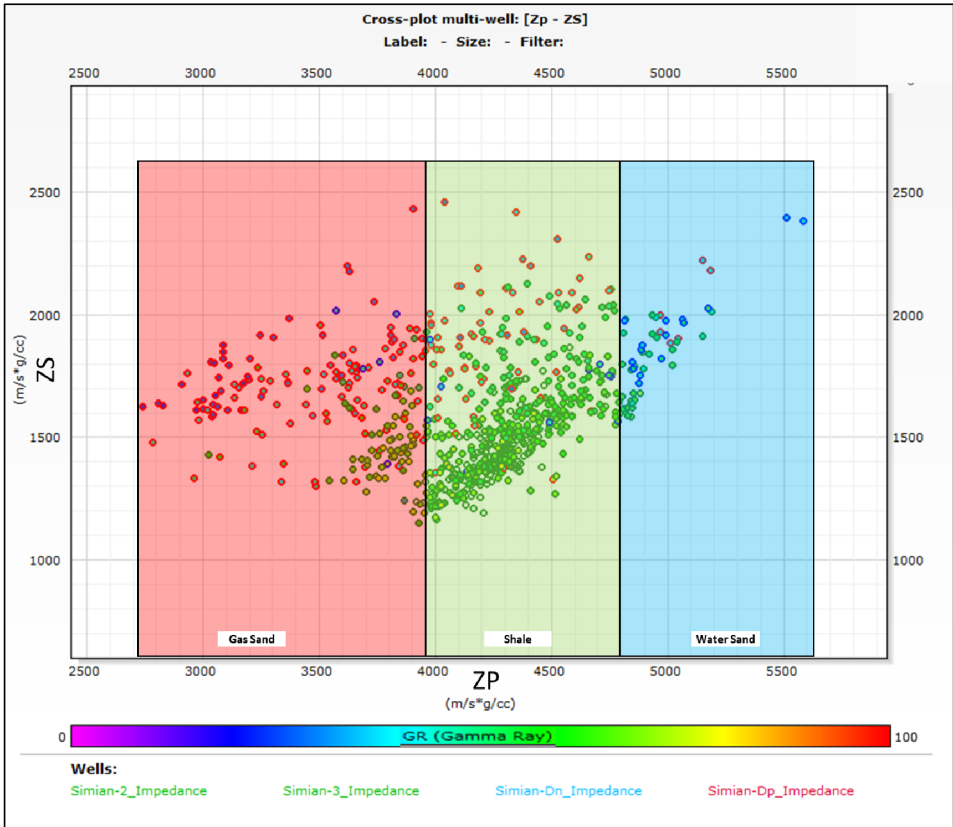


Fig. 8. Cross plot of Shear impedance (Zs) Vs compressional impedance (Zp) cross plot for separating Gas sand, shale and water sand facies.

resolution measured in tens of meters. Although porosity variations can be significant at the reservoir characterization scale, porosity maps derived from seismic data tend to reduce these fluctuations by averaging them vertically.

The estimated porosity logs were used to validate the developed porosity model, and the results matched where the areas with high porosity values are located in relation to the increasing porosity indicated by the log data. The porosity cube will be utilized as a trend cube for distribution of the porosity values, which will have a reliable impact on the static reservoir model. The inverted porosity model would be very helpful if used as a re-

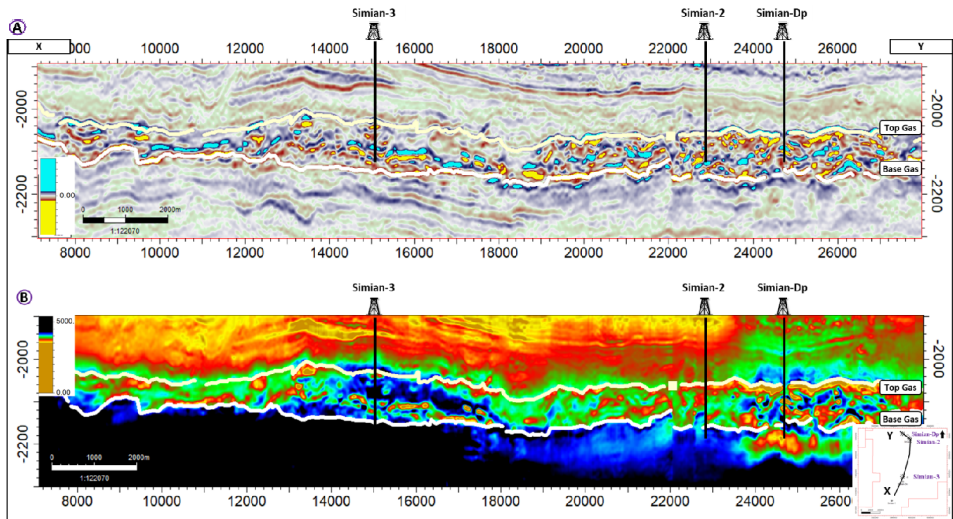


Fig. 9. (A) Representative seismic section in the study area; (B) Acoustic impedance cross section as a result of the Post Stack inversion generated for the location of the study wells (soft kick is represented by blue, while hard in red colour).

gional trend for delineating the areas with higher porosity values due to the method’s limitation.

This limitation is related to the differences in scale/sampling rate between the seismic and the well (Fig. 12). In order to validate the expected porosity values away from the wells in the predicted model, a blind well (Simian-1) was employed with significant results as shown in Fig. 13. A certain porosity maps including the maximum amplitude of porosity and the sum of porosity magnitude (Fig. 14) were constructed to identify the best locations for the future drilling wells. The created maps exhibit the same depositional trends in the region identically similar to the channel (Fig. 10). Apparently, the porosity increases in the northern sector if compared to the southern sectors.

5. Discussion

Porosity estimation from seismic inversion is a commonly used technique in geophysics to predict subsurface porosity based on seismic data. Seismic

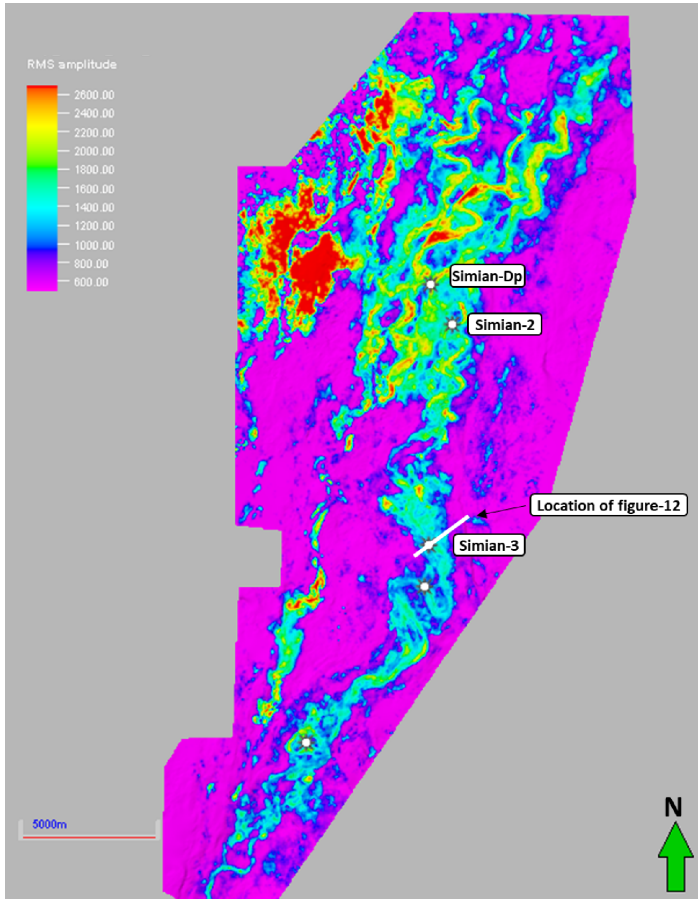


Fig. 10. Root mean square (RMS) amplitude from the top to base gas sand using full stack seismic.

inversion is the process of converting seismic reflection data into a quantitative representation of subsurface properties.

Porosity is a measure of the void spaces or gaps within a rock formation and is a critical parameter for assessing reservoir potential and fluid storage capacity. It directly influences the flow of fluids such as oil, gas, and water within the subsurface. Seismic inversion methods aim to relate the seismic response (amplitude, phase, frequency content) to rock properties such as porosity. A rock physics model is created to establish the relationship

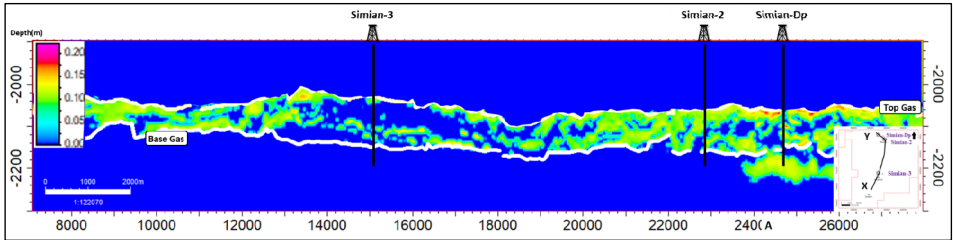


Fig. 11. Distribution of effective porosity estimated using the relationship established between porosity and AI.

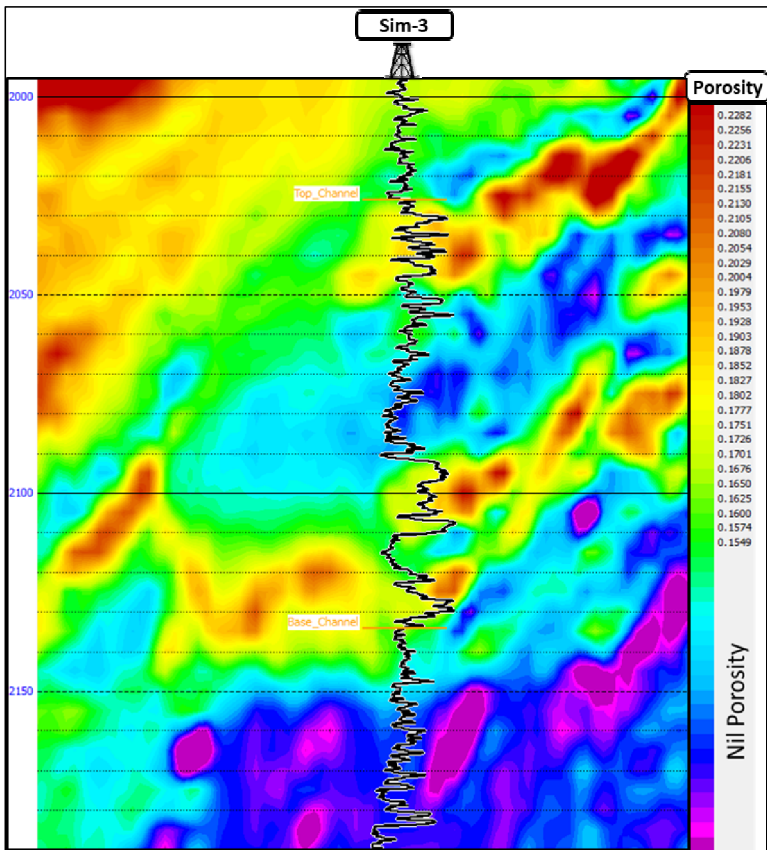


Fig. 12. Porosity cross section through Sim-3. The black curve is the density calculated porosity log, hot colours represent sand reservoir and pale represent background. For the location see Fig. 10. Nil means zero effective porosity in shale.

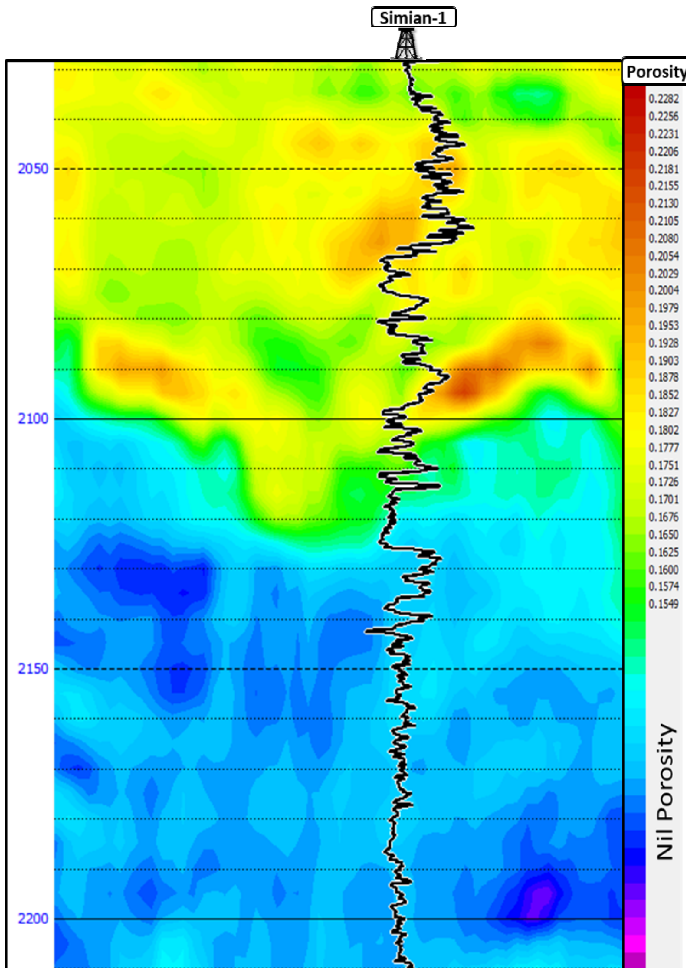


Fig. 13. Porosity cross section through Simian-1 as a blind testing well in the study area, the black curve is the density calculated porosity log.

between seismic response and porosity. This model incorporates information about the elastic properties of the rock, pore fluid properties, and the porosity-permeability relationship. The model can be derived from well log data.

The inversion process utilizes algorithms to invert the seismic data and estimate the subsurface properties. Different inversion techniques exist, in-

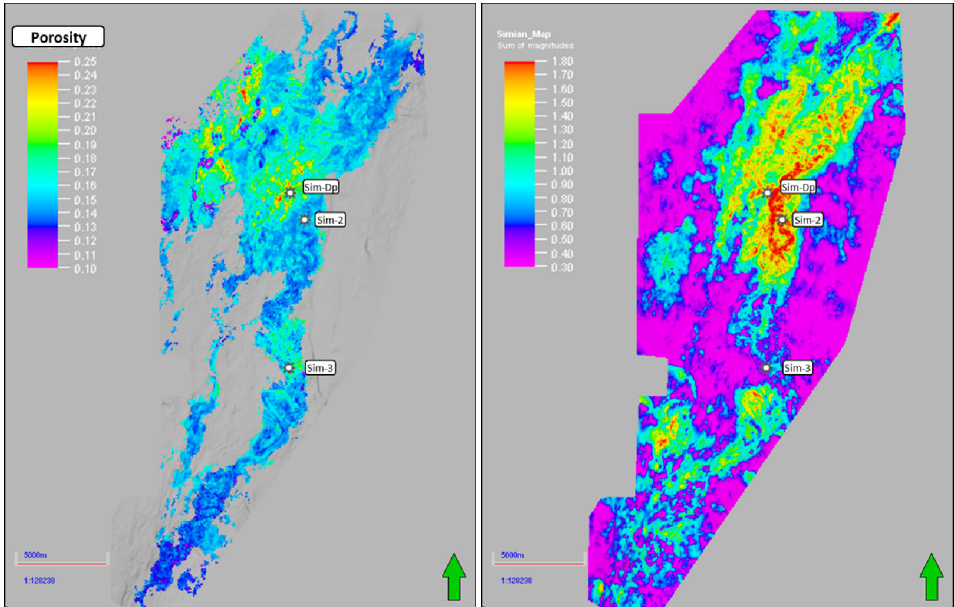


Fig. 14. Maximum amplitude (left) from the calculated porosity volumes and sum of magnitude (right) from the post-stack seismic from top to base of the reservoir section.

cluding deterministic, probabilistic, and model-based approaches. These methods attempt to find the best-fit model that reproduces the observed seismic data by adjusting the parameters, such as porosity, within the rock physics model. The inverted porosity model is validated against well log data or other independent measurements like porosity from the core to assess its accuracy and reliability. If necessary, additional adjustments or calibration may be performed to improve the porosity estimation.

It is important to note that porosity estimation from seismic inversion is subject to uncertainties and limitations. The accuracy of the results depends on factors such as the quality and resolution of the seismic data, the reliability of the rock physics model, and the presence of other geological complexities that may affect porosity distribution.

Overall, seismic inversion provides a valuable tool for estimating porosity from seismic data, allowing geoscientists and reservoir engineers to make informed decisions regarding resource exploration and production strategies.

6. Conclusion

Seismic inversion is a widely employed geophysical technique that enables the estimation of subsurface porosity based on seismic data. It involves the conversion of seismic reflection data into a quantitative representation of subsurface properties.

Porosity serves as a measure of the void spaces or gaps within a rock formation and plays a crucial role in evaluating reservoir potential and fluid storage capacity. It directly influences the flow of oil, gas, and water within the subsurface. Seismic inversion methods aim to establish a connection between the seismic response (including amplitude, phase, and frequency content) and rock properties such as porosity.

To achieve this, a rock physics model is developed, which considers the elastic properties of the rock, properties of the pore fluid, and the relationship between porosity and permeability. This model can be derived from well log data, providing valuable insights into the subsurface properties.

The inversion process employs algorithms to invert the seismic data and estimate the underlying subsurface properties, including porosity. By comparing the seismic response with the rock physics model, the inversion algorithms work to find the most suitable subsurface property model that reproduces the observed seismic data.

Through the utilization of seismic inversion, geoscientists can gain valuable information about subsurface porosity and its impact on fluid flow dynamics. This knowledge aids in making informed decisions in various applications, such as resource exploration and reservoir management.

We utilized post-stack seismic inversion products, specifically Z_p , for estimating porosity. Initially, we calculated the porosity at the drilled well locations and created a cross-plot comparing the raw acoustic impedance data with the calculated porosity. This cross-plot allowed us to observe the correlation between these two variables. Subsequently, we employed the correlation equation to convert the inverted post-stack seismic data (Z_p) into porosity values. To validate the accuracy of the new porosity volume, we tested it using a blind well and obtained reasonable results. The newly derived porosity cube will serve as a valuable tool for constructing reservoir static models. It will provide guidance on areas with both increased and decreased porosity, such as the central regions of the channels, which indi-

cate a high-quality reservoir in the core of slope channels. Additionally, the porosity shows an increasing trend towards the northern parts.

When a strong correlation exists between log porosity and acoustic impedance, porosity estimated through inversion can be utilized to analyse reservoir heterogeneities and identify promising areas distant from well data. It is important to note that while the inverted model can capture lateral variations effectively, the lower vertical resolution of seismic data, compared to well log data, leads to smoother vertical fluctuations. To handle finer vertical resolution necessary for reservoir simulation, simulation or stochastic techniques based on property distribution might be more suitable. To ensure reliable and robust conclusions when employing seismic inversion for porosity prediction, the availability of a rock physics model and correlation model specific to the study area is imperative. Seismic inversion has demonstrated its capability to accurately predict reservoir porosity.

Acknowledgements. The authors thank Rashid Petroleum Company (RASH-PETCO) and the Egyptian General Petroleum Corporation (EGPC) for providing the data, and permission to publish this study.

References

- Abbas A., Zhu H., Anees A., Ashraf U., Akhtar N., 2019: Integrated seismic interpretation, 2D modeling along with petrophysical and seismic attribute analysis to decipher the hydrocarbon potential of Missakeswal area. *Pakistan. J. Geol. Geophys.*, **8**, 1, 1000455, doi: 10.4172/2381-8719.1000455.
- Abdolahi A., Chehrazi A., Kadkhodaie A., Babasafari A. A., 2022: Seismic inversion as a reliable technique for anticipating of porosity and facies delineation, a case study on Asmari Formation in Hendijan field, southwest part of Iran. *J. Pet. Explor. Prod. Technol.*, **12**, 11, 3091–3104, doi: 10.1007/s13202-022-01497-y.
- Ali M., Jiang R., Ma H., Pan H., Abbas K., Ashraf U., Ullah J., 2021: Machine learning – A novel approach of well logs similarity based on synchronization measures to predict shear sonic logs. *J. Pet. Sci. Eng.*, **203**, 108602, doi: 10.1016/j.petro1.2021.108602.
- Ali S. A., Farag K. S. I., Ewida H. F., Mahdy A. M. A., 2019: Porosity prediction from the post-stack seismic inversion results of the sand channels at Simian gas field, Egypt's offshore west Nile delta. *Egyptian Geophysical Society, EGS Journal*, **17**, 1, 167–174.
- Ashraf U., Zhu P., Yasin Q., Anees A., Imraz M., Mangi H. N., Shakeel S., 2019: Classification of reservoir facies using well log and 3D seismic attributes for prospect evaluation and field development: A case study of Sawan gas field, Pakistan. *J. Petr. Sci. Eng.*, **175**, 338–351, doi: 10.1016/j.petro1.2018.12.060.

- Barakat M., Dominik W., 2010: Seismic Studies on the Messinian Rocks in the Onshore Nile Delta, Egypt. 72nd EAGE Conference and Exhibition incorporating SPE EUROPEC 2010, Barcelona, Spain, 14–17 June 2010, cp-161-00770, doi: 10.3997/2214-4609.201401362.
- Barakat M. Kh., El-Gendy N., El-Nikhely A. Zakaria A., Hellish H., 2021: Challenges of the seismic image resolution for gas exploration in the East Mediterranean Sea. *J. Pet. Min. Eng.*, **23**, 2, 13–23, doi: 10.21608/JPME.2021.86935.1092.
- Coulon J.-P., Lafet Y., Deschizeaux B., Doyen P. M., Dubois P., 2006: Stratigraphic Elastic Inversion for Seismic Lithology Discrimination in a Turbiditic reservoir. 76th SEG Annual International Meeting, Expanded Abstracts, 2092–2096, doi: 10.1190/1.2369949.
- Cowan G., Swallow J., Charalambides P., Lynch S., Dearlove M., Sobhani K., Nashaat M., Loudon E., Maddox S., Coolen P., Houston R., 1998: The Rosetta P1 field: A fast track development case study, Nile Delta, Egypt. *Egyptian General Petroleum Corporation Exploration & Production Conference Proceedings*, **1**, 222–235.
- Cross N. E., Cunningham A., Cook R. J., Taha A., Esmaie E., El Swidan N., 2009: Three-dimensional seismic geomorphology of a deep-water slope-channel system: The Sequoia field, offshore West Nile Delta, Egypt. *Am. Assoc. Pet. Geol. Bull.*, **93**, 8, 1063–1086, doi: 10.1306/05040908101.
- Deibis S., Futyan A. R., Ince D. M., Morley R. J., Seymour W. P., Thompson S., 1986: The stratigraphic framework of the Nile Delta and its implications with respect to the region's hydrocarbon potential. In: 8th EGPC Petroleum Exploration and Production Conference, Cairo, Egypt, 164–174.
- Dolson J. C., Boucher P. J., Siok J., Heppard P. D., 2005: Key challenges to realizing full potential in an emerging giant gas province: Nile delta/Mediterranean offshore, deep water, Egypt. In: Doré A. G., Vining B. A. (Eds.): *Petroleum Geology: North-West Europe and global perspectives*, Proceedings of the 6th Petroleum Geology conference the Geological Society London, 607–624.
- Dolson J. C., Shann M. V., Matbouly S., Harwood C., Rashed R., Hammouda H., 2001: The petroleum potential of Egypt (chapter 23). In: Downey M. W., Threet J. C., Morgan W.A. (Eds.): *Petroleum provinces of the twenty-first century*, *Am. Assoc. Pet. Geol. Mem.*, **74**, 453–482.
- Duval B. C., Cramez C., Vail P. R., 1998: Stratigraphic cycles and major marine source rocks. In: De Graciansky P.-C., Hardenbol J., Jacquin T, Vail P. R. (Eds.): *Mesozoic and Cenozoic sequence stratigraphy of European Basins*. Society for Sedimentary Geology, Special Publication, **60**, 43–51, doi: 10.2110/pec.98.02.0043.
- Eid R., El-Anbaawy M., Abdelhalim A., 2020: Integrated seismic and well gamma-ray analysis for delineation Sienna channel depositional architecture, offshore West Nile Delta, Egypt. *NRIAG J. Astron. Geophys.*, **9**, 1, 563–571, doi: 10.1080/20909977.2020.1820267.
- El-Gendy N. H., Radwan A. E., Waziry M. A., Dodd T. J. H., Barakat M. Kh., 2022: An integrated sedimentological, rock typing, image logs, and artificial neural networks analysis for reservoir quality assessment of the heterogeneous fluvial-deltaic Messinian Abu Madi reservoirs, Salma field, onshore East Nile Delta, Egypt. *Marine*

- and Petroleum Geology, *Mar. Pet. Geol.*, **145**, 105910, doi: 10.1016/j.marpetgeo.2022.105910.
- El-Nikhely A., El-Gendy N. H., Bakr A. M., Zawra M. S., Ondrak R., Barakat M. Kh., 2022: Decoding of seismic data for complex stratigraphic traps revealing by seismic attributes analogy in Yidma/Alamein concession area Western Desert, Egypt. *J. Pet. Explor. Prod. Technol.*, **12**, 12, 3325–3338, doi: 10.1007/s13202-022-01527-9.
- Helal A. N. M. A., Farag K. S. I., Hosny A., 2014: Use of 3D Post-stack Seismic Inversion for Quantitative Subsurface Interpretation at Simian Gas Field, Egypt's Offshore West Nile Delta, Egypt. *Egypt. J. Pure & Appl. Sci.*, 2014; **52**, 1, 29–35.
- Lindseth R. O., 1979: Synthetic sonic logs—a process for stratigraphic interpretation. *Geophysics*, **44**, 1, 3–26, doi: 10.1190/1.1440922.
- Mitchum R. M., Sangree J. B., Vail P. R., Wornardt W. W., 1993: Recognizing sequences and systems tracts from well-logs, seismic data, and biostratigraphy: examples from the late Cenozoic. In: Posamentier H. W., Weimer P. (Eds.): *Siliciclastic sequence stratigraphy: recent development and applications*. Am. Assoc. Pet. Geol. Mem., **58**, AAPG Special Volume, 163–198.
- Othman A. A. A., Metwally F., Fathy M., Said W., 2020: Reservoir characterization utilizing pre-stack inversion and artificial neural network techniques, Offshore Nile Delta, Egypt. *First Break*, **38**, 12, 37–42, doi: 10.3997/1365-2397.fb2020086.
- Pendrel J., 2006: Seismic inversion – still the best tool for reservoir characterization. *CSEG Rec.*, **31**, 1, 5–12.
- Russell B., Hampson D., 1991: Comparison of post-stack seismic inversion methods. *SEG Annual International Meeting, Expanded Abstracts*, 876–878, doi: 10.1190/1.1888870.
- Samuel A., Kneller B., Raslan S., Sharp A., Parsons C., 2003: Prolific deep-marine slope channels of the Nile Delta, Egypt. *Am. Assoc. Pet. Geol. Bull.*, **87**, 4, 541–560, doi: 10.1306/1105021094.
- Schlumberger, 1987: *Log interpretation Principles/Applications*. Schlumberger Education Service, Houston, Texas, 69–94.
- Sehim A., Hussein M., Kasem A., Shaker A., Swidan N., 2002: Structural architecture and tectonic synthesis Rosetta Province, West Nile Delta Mediterranean. In Egypt, presented at Mediterranean offshore conference (MOC), Alexandria.
- Tonn R., 2002: Neural network seismic reservoir characterization in a heavy oil reservoir. *Lead. Edge*, **21**, 3, 309–312, doi: 10.1190/1.1463783.
- Weimer P., Slatt R., 2004: *Petroleum Systems of Deepwater Settings*. Society of Exploration Geophysicists and the European Association of Geoscientists and Engineers, 1-1 to 1-15, 2-1 to 2-38, 4-1 to 4-87 and 5-1 to 5-48, 490 p.
- Wood H., O'Neill A., Cook R., Nigel B., 2012: An investigation into Messinian Prospectivity in the WDDM Concession, Offshore Nile Delta, Egypt. Imperial College, London, 120 p.